Blending Chitosan with Polycaprolactone: Effects on Physicochemical and Antibacterial Properties

Aparna R. Sarasam,[†] Raj K. Krishnaswamy,[‡] and Sundararajan V. Madihally*[,†]

School of Chemical Engineering, Oklahoma State University, Stillwater, Oklahoma 74078, and Chevron Phillips Chemical Company, Bartlesville Technology Center, Bartlesville, Oklahoma 74004

Received December 8, 2005; Revised Manuscript Received March 2, 2006

Chitosan is a well sought-after polysaccharide in biomedical applications and has been blended with various macromolecules to mitigate undesirable properties. However, the effects of blending on the unique antibacterial activity of chitosan as well as changes in fatigue and degradation properties are not well understood. The aim of this work was to evaluate the anti-bacterial properties and changes in physicochemical properties of chitosan upon blending with synthetic polyester poly(ϵ-caprolactone) (PCL). Chitosan and PCL were homogeneously dissolved in varying mass ratios in a unique 77% acetic acid in water mixture and processed into uniform membranes. When subjected to uniaxial cyclical loading in wet conditions, these membranes sustained 10 cycles of predetermined loads up to 1 MPa without break. Chitosan was anti-adhesive to Gram-positive *Streptococcus mutans* and Gram-negative *Actinobacillus actinomycetemcomitans* bacteria. Presence of PCL compromised the antibacterial property of chitosan. Four-week degradation studies in PBS/lysozyme at 37 °C showed initial weight loss due to chitosan after which no significant changes were observed. Molecular interactions between chitosan and PCL were investigated using Fourier transform infrared spectroscopy (FTIR) which showed no chemical bond formations in the prepared blends. Investigation by wide-angle X-ray diffraction (WAXD) indicated that the crystal structure of individual polymers was unchanged in the blends. Dynamic mechanical and thermal analysis (DMTA) indicated that the crystallinity of PCL was suppressed and its storage modulus increased with the addition of chitosan. Analysis of surface topography by atomic force microscopy (AFM) showed a significant increase in roughness of all blends relative to chitosan. Observed differences in biological and anti-bacterial properties of blends could be primarily attributed to surface topographical changes.

1. Introduction

Owing to its biocompatibility, biodegradability into nontoxic products, and antimicrobial properties, chitosan has been a much sought after material in a variety of applications including biomedical devices, wound healing, controlled drug delivery,[1] and food packaging[2] in the past 20 years. It has also sparked interest in the field of tissue engineering as a scaffold material due to added advantages such as processability into desired porous configurations,[3] positive charge and reactive functional groups that help interact with other molecules, low cost and easy availability. Chitosan has already been investigated in the regeneration of skin,[4] cartilage,[5] nerve,[6] bone,[7] liver,[8] and periodontal tissues.[9−11] Utilizing bactericidal properties of chitosan against numerous pathogenic microorganisms,[12−14] coating prosthetic grafts with chitosan has also been attempted to combat post-operative infection.[15] Despite these advances, current use in tissue engineering is limited mainly by the low strength and incomplete understanding of the cellular interaction with chitosan.

Several approaches have been taken to overcome the limitations of chitosan, including graft polymerization[16,17] and blending[18−20] with other natural or synthetic polymers. Polymer blends have shown favorable results in terms of the targeted biological, mechanical or degradation properties in comparison to the individual components. Blending with poly(ϵ-caprolactone) (PCL) is an attractive option due to its flexibility in combining with other polymers facilitated by its low melting point (60 °C) and glass transition temperature (−60 °C). It is a biodegradable and biocompatible polyester with excellent tensile properties.[21] However, PCL usage in biomedical applications has been restricted to controlled rate drug delivery[22] and medical devices such as sutures and catheters.[23] In tissue engineering, PCL suffers the disadvantages of (1) poor bioregulatory activity primarily due to its highly hydrophobic nature, (2) slow rate of biodegradation, and (3) susceptibility to microbial action. Nevertheless, the versatility of PCL in blending with other polymers allows the modification of its properties to overcome its drawbacks.[24−26]

In our previous study, chitosan and PCL were blended using a unique solvent, unlike other complex techniques.[21] Despite differences in their affinity to water, chitosan and PCL were homogeneously dissolved in 77% aqueous acetic acid in different mass ratios and processed into uniform membranes. Tensile testing of membranes showed alterable mechanical properties based on processing conditions and blend composition. Importantly, mouse embryonic fibroblasts showed better cell spreading and viability on blend membranes relative to pure chitosan or pure PCL membranes.

In this study, first the analysis was extended to assess the fatigue properties of chitosan in wet conditions and anti-bacterial properties in the presence of PCL against Gram-positive *Streptococcus mutans* (causes dental caries[27]) and Gram-negative *Actinobacillus actinomycetemcomitans* (causes various forms

* To whom correspondence should be addressed. Address: 423 Engineering North, School of Chemical Engineering, Oklahoma State University, Stillwater, OK 74078. Phone: (405) 744 9115. Fax: (405) 744 6338. E-mail: sundar.madihally@okstate.edu.

[†] Oklahoma State University.

[‡] Chevron Phillips Chemical Company.

10.1021/bm050935d CCC: $33.50
Published on Web 03/25/2006

of periodontitis[28]). Further, molecular interactions between chitosan and PCL and changes in their physicochemical properties were evaluated. In particular, changes in crystal structure, dynamic thermomechanical behavior, and surface topographies were analyzed by WAXD, DMTA, and AFM, respectively. These polymers degrade by different mechanisms; chitosan degrades into oligosaccharides by enzymatic action of lysozyme (maximum at pH 4.5−5.5),[29,30] whereas PCL undergoes nonenzymatic bulk hydrolysis of its ester linkage, followed by fragmentation into oligomers.[31] The degradation rate of synthetic polymers could increase with the addition of a natural component due to reduced crystallinity and hydrophobicity.[24,32] Since altered degradation rate could also play a role in observed biological activity, lysozyme-mediated degradation rates were also evaluated. Results suggest that increased biological activity on blends could be due to increased surface roughness of the membranes.

2. Experimental Methods

2.1. Materials. Chitosan (∼85% degree of deacetylation (DD)) of high molecular weight (MW >310 kD) and low MW (40−190 kD), polycaprolactone (PCL) of MW 80 kD, and hen egg white lysozyme (46400 U/mg) were purchased from Sigma Aldrich (St. Louis, MO). *Streptococcus mutans* (ATCC 25175, NCTC 10449) and *Actinobacillus actinomycetemcomitans* (ATCC 43719, NRRL 2501) bacteria were purchased from ATCC and grown for 48 h in brain heart infusion (BHI) broth at 37 °C in aerobic conditions. Cultures in their early growth phase were used for antibacterial experiments. All other chemicals used were of reagent grade.

2.2. Formation of Chitosan-PCL Blend Membranes. Chitosan and PCL were blended in three different mass ratios and processed into membranes as described previously.[21] In brief, 3 mL of chitosan solutions (2% w/v) dissolved in 0.5 M acetic acid were slowly added to 10 mL of 0.2%, 0.6%, and 1.8% PCL solutions dissolved in glacial acetic acid to obtain blends of 25%, 50%, and 75% PCL composition by mass, respectively. The mixtures were slightly warmed and stirred to form homogeneous solutions. These solutions were dried in Teflon dishes for 24 h in an oven at 55 °C to form uniform membranes of approximately 80−120 μm thickness.

2.3. Analysis of Fatigue Properties. Membranes were tested under wet 37 °C conditions[21] using an Instron 5542 testing machine under uniaxial cyclical loading as described previously.[33] Briefly, membranes were cut into 50 mm × 10 mm size strips, neutralized with 1 N NaOH, washed with water, and hydrated with phosphate buffer saline (PBS). A custom built chamber surrounding the grips with constant circulation of PBS maintained at 37 °C provided constant hydrating conditions. Under cyclical loading, the crosshead speed was kept constant at 10 mm/min and samples were strained repeatedly between two preset fluctuating loads for 10 cycles. The load limits were predetermined by the linear portion of the load-extension curves obtained previously under monotonic loading.[21] These limits were 0.2−2 N for chitosan (MW > 310 kD), 0.2−1 N for blends, and 0.2−8 N for PCL membranes. Additionally, the influence of MW was also studied by testing a low MW (50−190 kD) chitosan between loads 0.2−1 N.

2.4. Analysis of Antibacterial Properties. Membranes were cut into 20 mm × 20 mm size strips, neutralized and sterilized by immersion in 90% ethanol for 15 min, and washed thoroughly in sterile PBS. To test the bactericidal properties, membranes were suspended in 5 mL of bacterial broths of known optical density (OD) taken in small glass vials with rubber caps and incubated at 37 °C with constant gentle shaking. Transient changes in turbidity of the broths were measured in triplicate samples at 3, 6, 12, and 24 h by withdrawing 0.5 mL of broth, diluting to 1 mL with deionized water, and measuring the OD using a spectrophotometer at 600 nm wavelength. Suspension cultures without any membranes were used as control.

To analyze the adherence of bacteria, membranes were retrieved from cultures after 24 h and fixed in 3.7% paraformaldehyde for 30 min followed by washing with PBS. Membranes were air-dried in a vacuum desiccator for 24 h prior to sputter coating with gold for 1min and then observed under a JEOL 6360 scanning electron microscope (JEOL USA Inc., Peabody, MA). Images were obtained at representative locations.

2.5. Analysis of Lysozyme-Mediated Degradation Kinetics. These studies were conducted as reported previously[18] for a period of four weeks. Chitosan, 50% PCL, and pure PCL membranes were cut into 20 mm × 20 mm size strips, and their initial weights were measured. The strips were neutralized in 1 N NaOH, washed with deionized water, sterilized in absolute alcohol for 30 min, and washed thoroughly in sterile PBS prior to incubating in 10 mL PBS with and without (control) 100 mg/L HEW lysozyme. Incubations were carried out in 20 mL vials with a ∼15 mm diameter hole drilled in the caps and covered on the inside with 0.22 μm filters. Media was replaced every 2 days.

At two day intervals, three samples per group were sacrificed for degradation analysis and incubation media was collected for pH analysis. Sacrificed samples were washed with deionized water, dehydrated using absolute alcohol, and dried to constant weight in a vacuum desiccator at ambient conditions prior to final weight determination. Digital images were also obtained to characterize dimensional changes. Samples sacrificed after thirty minutes of incubation were considered as day zero samples.

2.6. Analysis of Molecular Interactions. Membranes were probed using a Thermo Nicolet IR300 FT-IR Spectrometer (Thermo Electron Corporation, Madison, WI). Samples were mounted on a film holder, and spectral scans of films were obtained at ambient conditions at a resolution of 4 cm^{-1} with an accumulation of 8 scans, using the associated EZ-OMNIC software. Peaks were analyzed by plotting the data in SigmaPlot 9 software (SPSS Science, Chicago, IL).

2.7. Analysis of Crystal Structure. Changes in crystal structure of chitosan and PCL in the blends were analyzed using a Rigaku-MSC wide-angle X-ray diffractometer (Rigaku/MSC, The Woodlands, TX) in D-MAX-A mode with an MDI databox. X-rays were generated using a 12kV rotating anode generator and the goniometer was rotated from 2° to 40° at a speed of 2°/min.

2.8. Analysis of Dynamic Mechanical Properties. Thermomechanical analysis was performed on dry membranes of 20 mm × 6 mm size using a Seiko DMS 200 DMTA. Samples were heated from −100 to +160 °C at a rate of 2 °C/min and measurements were made at 0.1, 1.0, and 10 Hz frequencies simultaneously in tension mode under nitrogen atmosphere. Changes in storage modulus (E') and loss factor (tan δ) were recorded. The peak heights of tan δ curve were calculated using SigmaPlot 9 software.

2.9. Analysis of Surface Topography. Surface analysis of membranes was done by atomic force microscopy (AFM) using a DI Nanoscope IIIA Multimode Scanning Probe Microscope (Digital Instruments, Veeco Metrology Group, Santa Barbara, CA) at ambient conditions. Sample films were attached onto iron AFM substrate disks using double-sided tape. Topographic images were obtained in tapping mode using commercial silicon microcantilever probes (MikroMasch, Portland, OR) with a tip radius of 5−10 nm and spring constant 2−5 N/m. The probe oscillation resonance frequency was ∼120 kHz and scan rate was 1 Hz. Images were captured at different locations, and the roughness factors were calculated using associated software (Nanoscope, version 5). The roughness factor R_q is the root-mean-square average of "n" number of height deviations (Z_i) taken from the mean data plane

$$R_q = \sqrt{Z_i^2/n}$$

2.10. Statistical Analysis. All experiments were repeated three or more times with triplicate samples for each group. Significant differences between two groups were evaluated using a one way analysis of

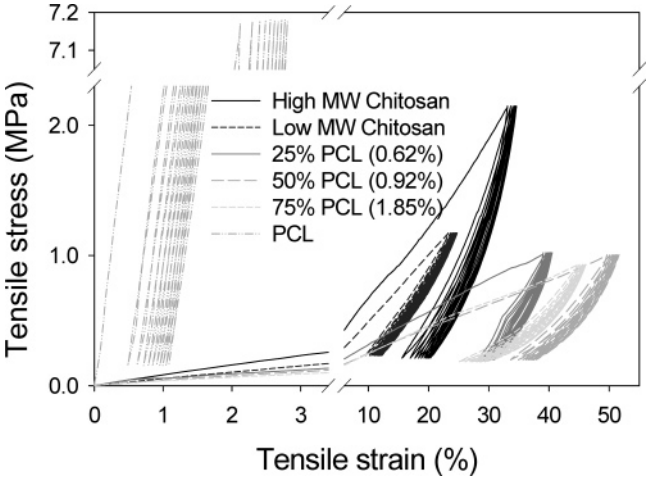

Figure 1. Effects of MW and blending with PCL on fatigue properties of chitosan membranes in simulated physiological conditions. Membranes were strained for 10 cycles between fixed load limits in a custom built chamber with PBS circulation at 37 °C. Numbers in brackets correspond to total polymer concentration in each blend.

variance (ANOVA) with 95% confidence interval. When $P < 0.05$, the differences were considered to be statistically significant.

3. Results

3.1. Effect of Blending on Fatigue Properties. First, when high MW chitosan membranes were subjected to fluctuating loads 0.2−2 N for 10 cycles, they did not break (Figure 1). Maximum deformation occurred in the first cycle and there was minimal deformation in subsequent cycles indicating no additional strain storage in the samples after the first cycle. Similarly, blend membranes and low MW chitosan membranes which were subjected to 10 cycles of loads 0.2−1 N, also withstood the stresses without breaking. PCL did not yield or elongate significantly within the specified load limits. However, blend membranes exhibited at least 10% higher strain than chitosan despite lower load limits and the strain values increased with increased PCL content. Among the blends, 50% PCL membrane showed maximum strain.

3.2. Effect of Blending on Antibacterial Properties. The bactericidal properties of chitosan against Gram-positive *S. mutans* were tested by suspending the membrane in bacterial broth and incubating at appropriate conditions. Transient changes in optical density (Figure 2) of the broth indicated that, except for 50% PCL, all of the biomaterials showed a decreased growth of bacteria in suspension when compared to the control. There were no significant differences in the optical densities of 25% and 75% PCL suspensions. At any given time, suspensions containing chitosan membranes showed the least growth of bacteria. Nevertheless, the growth of bacteria in the presence of these membranes indicated that chitosan, PCL, or their blends are not bactericidal. When the experiments were repeated with Gram-negative *A. actinomycetemcomitans* (Figure 2), growth was observed in suspensions of all membranes, including chitosan indicating that they were not bactericidal to this pathogen either. Nevertheless, in comparison to other groups, chitosan showed lower growth rates of *A. actinomycetemcomitans*, similar to *S. mutans*. Interestingly, unlike *S. mutans*, the growth rates in the presence of these membranes were higher than in the control. This indicated that the antibacterial activity of chitosan was more effective against *S. mutans* than against *A. actinomycetemcomitans* in suspensions.

When the adhesion of *S. mutans* to the membranes was observed under SEM, results (Figure 2) indicated that there was negligible adhesion on chitosan membranes. Presence of PCL increased bacterial adhesion significantly on the membranes. Similar results were observed with *A. actinomycetemcomitans* (Figure 2). On the 75% PCL membrane, chains of rod-shaped *A. actinomycetemcomitans* were fragmented due to cracking of underlying substrate during sample preparation for SEM, indicating that probably bacteria adhered strongly to the membranes.

3.3. Lysozyme-Mediated Degradation in Vitro. There was negligible weight loss in PCL membranes over the study period (Figure 3A), irrespective of the presence of lysozyme. Chitosan membranes showed maximum weight loss (20%) within the first 30 min which did not change much over the remaining study period. Similar to chitosan, 50% PCL showed significant weight loss (15%) within the first 30 min itself, indicating that the weight loss could be due to loss of chitosan. The effect of lysozyme on degradation was not significant in any group. Interestingly, dimensional changes in all membranes were negligible (data not shown), irrespective of composition or presence of lysozyme.

When pH of incubation media was analyzed, a decrease from the initial value of 7.4 was observed in all groups (Figure 3B). At any measured time point, pH of media containing PCL was the lowest, followed by 50% PCL and chitosan, although not statistically significant. On day zero, there was a marginal increase in the pH of chitosan and 50% PCL sample media, despite thorough washing of NaOH neutralized membranes. This could be due to a semistable binding of NaOH selectively to chitosan.

3.4. Molecular Interactions. Interferograms are presented in three frequency ranges in Figure 4A showing the typical absorption peaks of the functional groups present in chitosan and PCL.[34,35] These peaks were also observed in all of the blend interferograms although with varying intensities based on their composition. Characteristic peaks of chitosan were more distinguishable in 25% PCL, whereas those of PCL were better expressed in 50% and 75% PCL blends. The amine group of chitosan could potentially form an amide bond with the carbonyl group of ester groups in the chain or carboxylic acid groups at the end of chains of PCL (Figure 4B). In such a case, the absorption peak of carbonyl stretch would shift from 1725 cm^{-1} to a lower value (approximately 1630−1680 cm^{-1}) and the two peaks corresponding to amine group of chitosan would convert to one weak band as the primary amine changes to secondary form. These changes were not observed in the blend interferograms ruling out the possibility of the amide bond formation. The C−N bond stretch in the possible amide bond could not be distinguished from the existing C−N bonds in chitosan at 1000−1350 cm^{-1}.[36] These results implied that there was no detectable chemical bonding between chitosan and PCL in the formed blends, but they only coexisted.

3.5. Changes in Crystal Structure. The WAXD pattern of chitosan showed characteristic peaks (Figure 5A) at 10° and 20.5°.[37] Both the peaks appeared only in the 25% PCL blend and were broad and weak. The diffraction pattern of PCL (Figure 5B) showed sharp and well-defined characteristic peaks at 21.5°, 22°, and 23.5°.[38] These peaks were present in the 75% PCL pattern at the same angles with slightly reduced intensity. Fifty percent PCL blend (Figure 5A) showed all peaks of PCL as well as the chitosan peak at 10°, although with much reduced intensity. An absence of any additional peaks or shift in the diffraction angles indicated that the crystal structure of chitosan

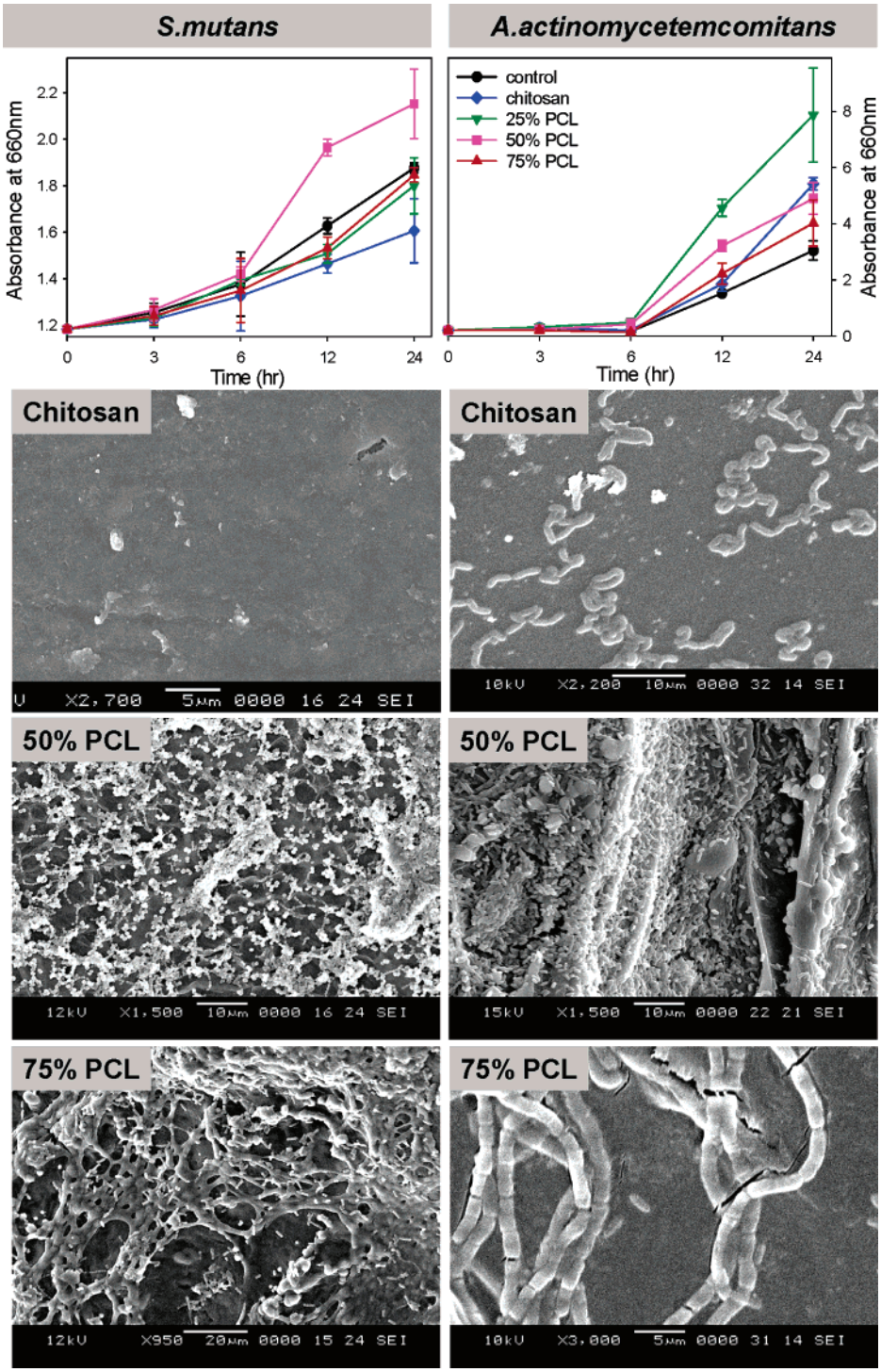

Figure 2. Effect of blending on anti-bacterial properties of Chitosan. Chitosan, PCL, and blend membranes were suspended in bacterial broths of *S. mutans* and *A. actinomycetemcomitans* and incubated aerobically at 37 °C. Transient changes in optical density of broth were measured and membranes were analyzed by SEM for bacterial adhesion.

and PCL is unchanged in the blends. The crystal structure of blends was influenced by the dominant component; that is, 25% PCL was similar to chitosan, whereas 50% and 75% PCL had similar structure to PCL.

3.6. Dynamic Mechanical and Thermal Properties. Chitosan undergoes thermal decomposition at 270 °C prior to melting and its glass transition temperature (T_g) is unclear. On the other hand, PCL has a sharp melting point of 60 °C and T_g near −60 °C. DMTA analysis showed the glass transition (α-relaxation) of PCL dissolved in acetic acid at −35 °C when it was heated from −100 to +50 °C (Figure 6A). There was no significant shift in the T_g of PCL in the blends indicating that the crystal structure of PCL may not be affected by the current method of blending with chitosan. However, the damping loss (tan δ) associated with glass transition of PCL decreased with PCL content as evident from reduced height of the peaks. This suggests that the crystallinity of PCL is suppressed in the blends. Storage modulus (E') of chitosan (Figure 6B) was 10 times higher than PCL due to its glassy/amorphous nature. The hardness (E') of ductile PCL which has flexible chains increased by the addition of brittle chitosan.

3.7. Surface Topography. When the surface morphology of membranes was probed with AFM, three-dimensional surface plots of height (Figure 7) showed that the chitosan surface was

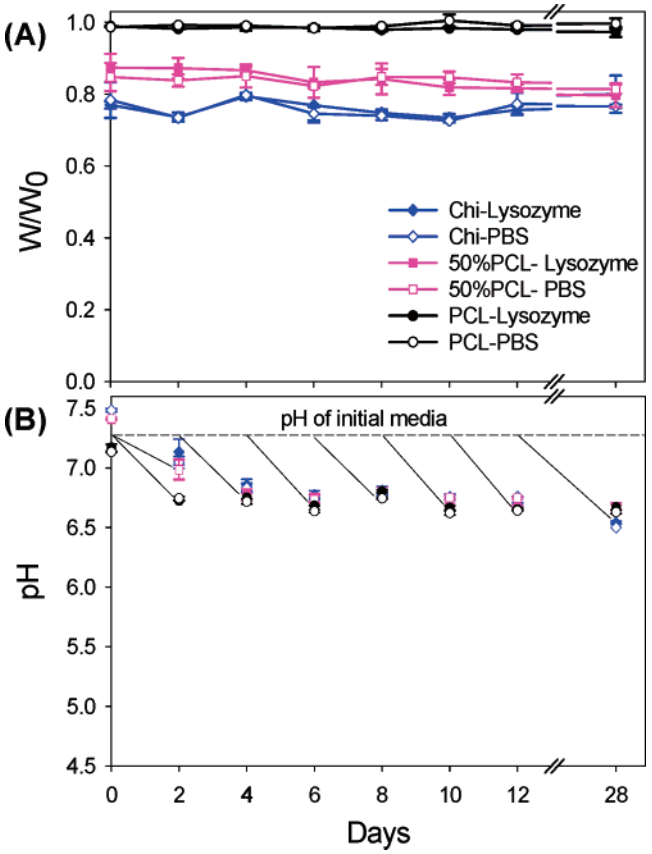

Figure 3. Effect of blending on degradation kinetics of chitosan and PCL. Membranes were incubated in PBS containing hen egg white lysozyme (100 mg/L) under sterile conditions at 37 °C. Transient changes in (A) weight loss and (B) pH.

smooth with uniformly distributed short spikes. Addition of PCL increased the height of these spikes. Seventy five percent PCL showed the tallest spikes over a large area, whereas pure PCL was smoother than 75% PCL. Interestingly, preferential orientation of fibers was visible in 25% and 50% PCL, which was absent on pure membranes, suggesting that the presence of two components influences each other's vertical and horizontal alignment. When roughness was analyzed, a significant increase in roughness factors was observed in all of the membranes containing PCL (Figure 7). Maximum roughness was observed in 75% PCL blends which was significantly higher than 25% or 50% PCL blends.

4. Discussion

Blending hydrophilic chitosan with hydrophobic PCL represents a good model for understanding blends of two semicrystalline polymers. Previously, we reported the possibility of blending chitosan and PCL in a single phase using a unique acetic acid solution without complex chemical modifications.[21] Formed blends showed that the solvents used did not cause toxicity to fibroblasts under in vitro testing conditions. Further, 50% and 75% PCL blends showed better support for mouse embryonic fibroblast spreading and survival relative to individual polymers. Measured tensile testing under monotonic loading showed that the tensile properties of blend membranes were dependent on the composition and processing conditions such as drying temperature, humidity, and chloroform annealing, thus demonstrating the possibility of altering the mechanical properties of chitosan.

In this study, the analyses were extended to include fatigue properties and the effect on the antibacterial properties of chitosan. Unlike monotonic loading, the effect of MW of chitosan was not significant under cyclical loading in the tested load range. All materials showed maximum deformation in the first cycle, suggesting that they could endure many more cycles. However, the tested membranes had changes in mass ratios of two polymers as well as the total concentration. As the packing density of polymers varies with total concentration, it may have significant influence on mechanical properties. Therefore, blend membranes of varying PCL composition were made with fixed total polymer concentration (0.62%) and tested (data not shown). Results indicated that varying total polymer concentration altered only the monotonic tensile properties and did not significantly influence the fatigue properties (hysteresis behavior). Hence, it may be concluded that at any total polymer concentration, the mass ratios of polymer components have a major influence on mechanical properties. Further analysis is necessary to understand the influence of total polymer concentration on other

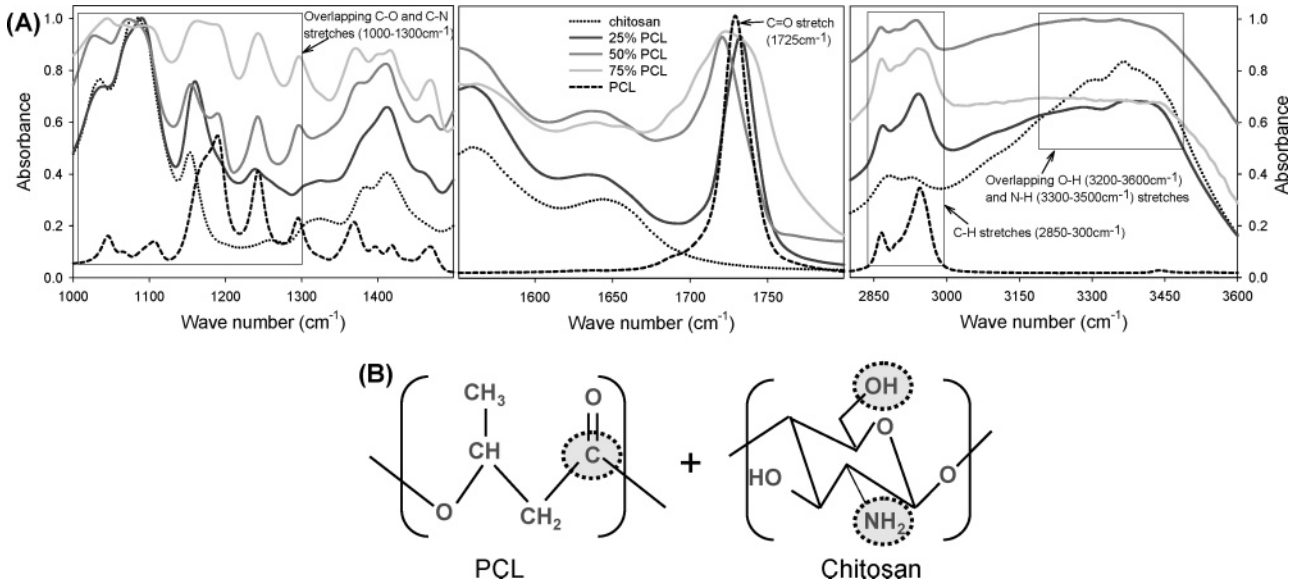

Figure 4. Molecular interactions between chitosan and PCL. (A) FTIR spectra of membranes at various frequencies obtained at ambient conditions at a resolution of 4 cm^{-1} and (B) Molecular structures of chitosan and PCL and scheme of possible bond formation between them.

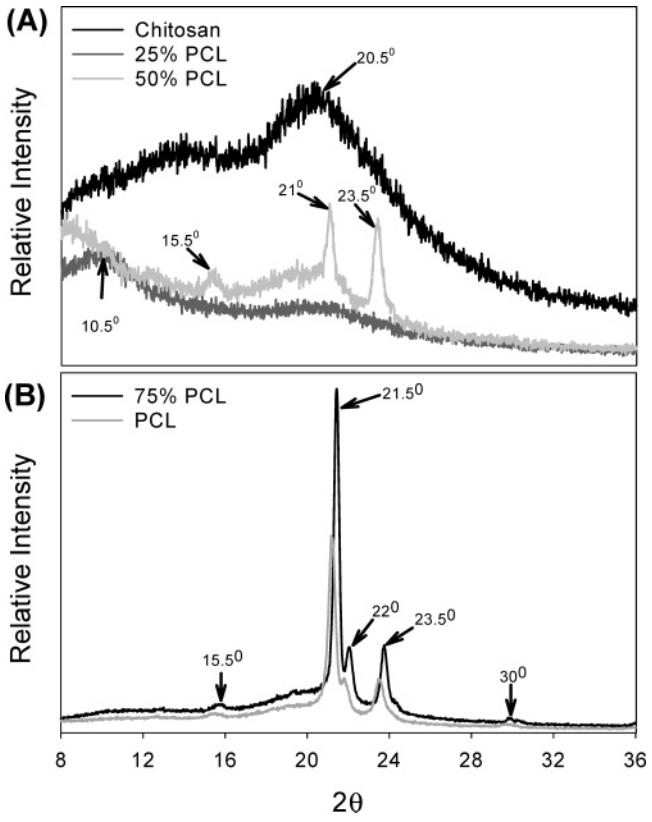

Figure 5. Effects of blending on crystal structure of Chitosan and PCL. Wide-angle X-ray diffraction patterns of membranes obtained with goniometer rotation from 2° to 40° at a speed of 2°/min. (A) Chitosan, 25% PCL, 50% PCL and (B) PCL, 75% PCL.

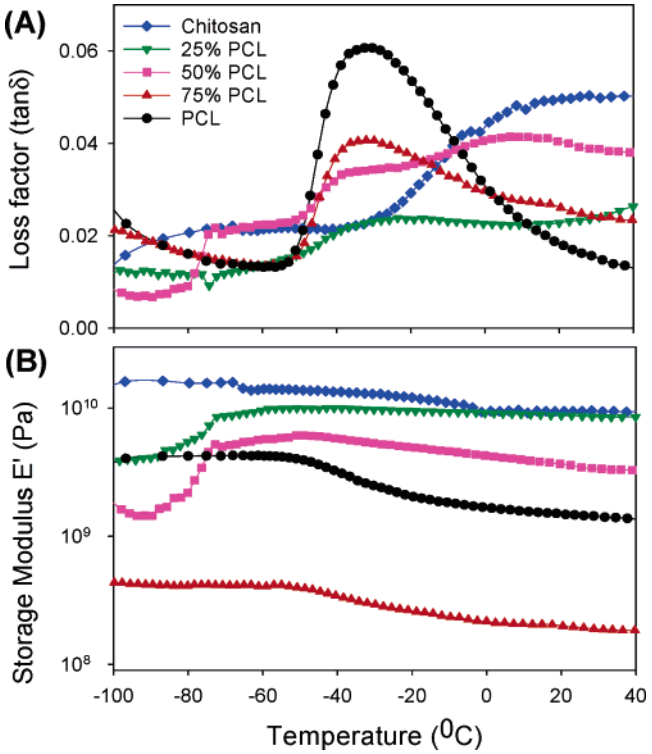

Figure 6. Dynamic thermomechanical properties of chitosan/PCL blend membranes by DMTA. Membranes were heated from −100 to +160 °C at a rate of 2 °C/min and an oscillating frequency of 10 Hz. (A) Loss factor and (B) storage modulus.

aspects of fatigue properties such as energy loss per hysteresis loop and strain per cycle. In addition, the analysis should be extended to determine the fatigue life (number of cycles of fluctuating stress and strain endured before permanent structural change) and fatigue limit (the maximum fluctuating stress endured for infinite cycles) of these polymers. Such information would help streamline these polymers for different biomedical applications.

When antibacterial properties were tested, chitosan was more potent against Gram-positive *S. mutans* than against Gram-negative *A. actinomycetemcomitans*, similar to literature reports.[39] Although the mechanism is not completely understood, it is believed that the positive charge on chitosan attracts and binds the negatively charged cell wall and causes cell lysis.[13] Bacterial studies also showed that the antibacterial property of chitosan may be contact dependent as it allows proliferation of bacteria away from it in suspension while inhibiting bacterial adhesion on its surface, similar to literature reports.[15] The antiadhesive properties of chitosan were compromised upon blending with PCL. A number of studies with other macromolecules have shown that chemical and mechanical properties of matrixes such as edges, grooves, hydrophilicity, presence of adhesion domains, roughness/nanotopographies, and stiffness influence cellular processes in two-dimensional (2D) matrixes.[40−43]

Since chitosan and PCL lack cell binding domains, the observed cellular response could be attributed to altered physicochemical properties. Thus, to understand the improved biological support of blends toward fibroblasts[21] and decreased antibacterial activity, first the degradation characteristics of the blends were tested. These results showed no significant difference between the blends and pure polymers. The degradation rate of chitosan was low despite a very high concentration of lysozyme, relative to physiological levels. This is attributed to the 85% DD chitosan used in this study as previous research has shown that highly deacetylated chitosan is less susceptible to lysozyme.[44] In addition, high MW PCL degrades slowly until the first stage of random hydrolytic chain scission which reduces the MW to 15 kD or less.[45] Hence, the observed alterations may not be due to degradation of these membranes. To understand the effect of degradation, forming blends with low MW PCL and chitosan with low degree of deacetylation is necessary.[46]

Chitosan is a poly(1,4-D-glucosamine) molecule with amine functional group which protonates in weak acids and provides chitosan its unique cationic nature. Analysis by FTIR indicated no new chemical bonds in the blends, suggesting that there was no chemical reaction between the two polymers, which is consistent with literature reports of PCL blends with other polysaccharides.[26] Other possible interactions include intermolecular hydrogen bonding between the oxygen atom of the carbonyl group of PCL and the hydrogen of the hydroxyl group or ammonium ion of chitosan, but they are not detectable by FTIR. Further studies are required to understand such interactions. Nevertheless, when the crystal structures were evaluated using WAXD, no changes were observed in the two polymers, suggesting that chitosan and PCL coexist as separate phases in the blends.

Previously, differential scanning calorimetry (DSC) studies showed a decrease in the melting temperature (T_m) of PCL with a decrease in PCL content in the blends.[21] Calculation of Flory−Huggins interaction parameters using the Nishi Wang approximation showed a concentration dependency and partial miscibility of the crystalline phase with the amorphous phase. Since the depression in melting point of PCL could be due to the noncrystalline phase acting as a diluent rather than altered crystal structure, this study evaluated the variations in T_g of

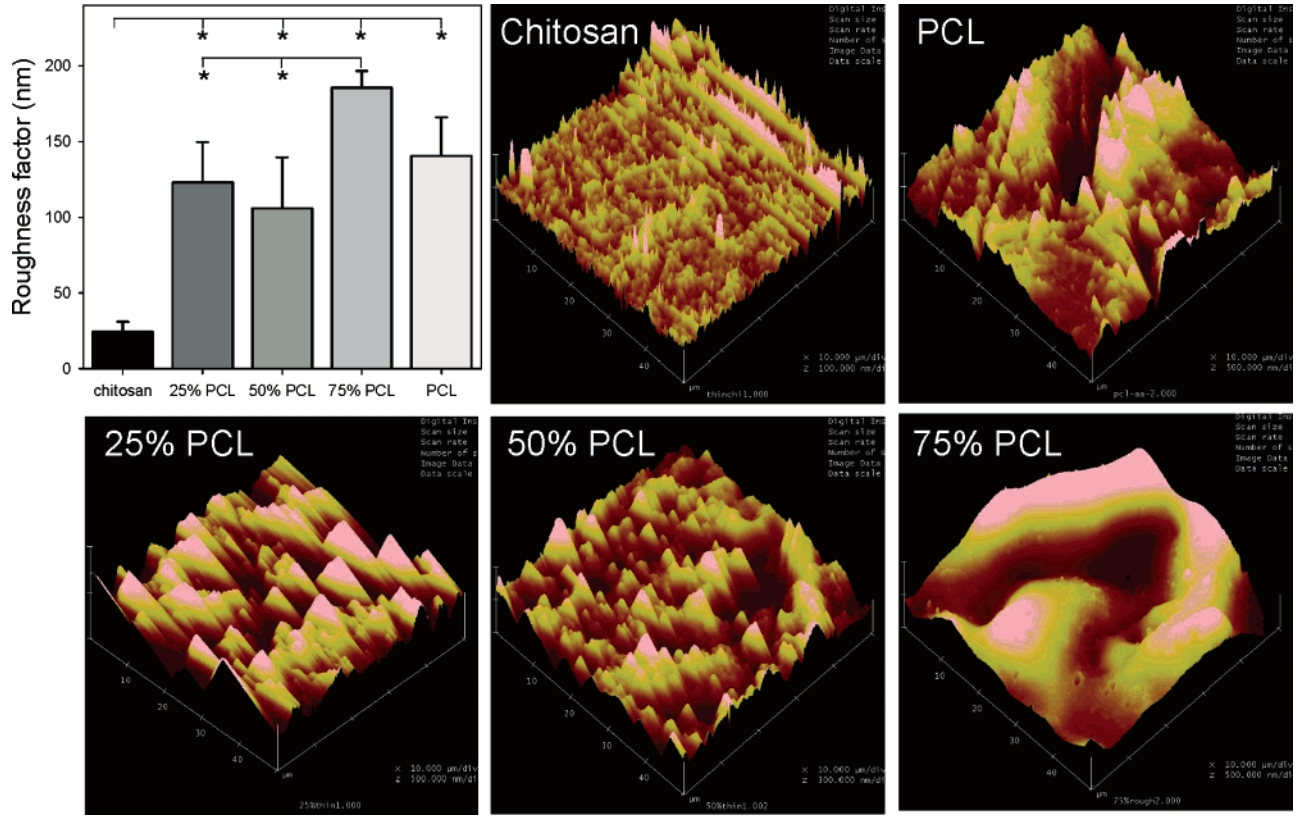

Figure 7. Effect of blending on surface morphology of membranes by AFM. Bar graphs showing roughness factors (*P < 0.05 between the indicated groups) and representative AFM height images obtained in tapping mode at a scan rate of 1 Hz.

PCL. First, no shift in the T_g of PCL in the blends reinforced that the PCL crystal structure did not change. Second, peak area under the T_g of PCL reduced with increasing diluent composition confirming that PCL crystallinity was suppressed by chitosan, similar to other polyester−polysaccharide blends.[26,47] However, these transitions were independent of each other without overlap in the relaxations confirming the findings from FTIR analysis that there was no chemical bonding between chitosan and PCL in the prepared blends. Thus, the observed alteration in adhesion of prokaryotic and eukaryotic cells may not be due to the altered crystal structures of the two polymers.

Analysis of surface topographies and roughness factors indicated that the blend surfaces were significantly rougher at the nanoscale than chitosan. Thus, the observed difference in cell adhesion could be partially attributed to the altered surface texture. However, altered hydrophilicities could also affect cell spreading as hydrophilicity influences the adsorption of proteins and prevents the adhesion of platelets and fibrinogen onto chitosan surface.[48,49] The presence of hydrophobic PCL could alter the hydrophilicity of chitosan resulting in the adsorption and binding of adhesive proteins in the extracellular matrix (ECM) of cells onto the biomaterial surface thus influencing the adherence and colonization of cells on blends. In other reports, we have also shown that the presence of poly(lactic-*co*-glycolic acid) hills on chitosan membranes decreased the cell spreading of fibroblasts and endothelial cells.[50] However, the observed changes in cellular activity could also be due to the decreased surface charge attributed to the shielding effect by PCL. Thus, one has to explore the changes in the surface charge density, hydrophilicity, and PCL distribution on the chitosan membrane. Blending with negatively charged molecules such as alginic acid or glycosaminoglycans would provide a better understanding of the charge-mediated anti-bacterial properties of chitosan.

In this study, blends were formed with nearly 4:1 chain length ratio of chitosan and PCL. Inverting this ratio would result in an altered packing assembly of chitosan and PCL fibers with the PCL chains forming the backbone. Such an orientation might make the chitosan molecules shorter and more accessible to lysozyme molecules resulting in accelerated degradation. The most significant impact would be felt on the surface topographical features of membranes with altered orientation of fibers. Thus, inverting the polymer chain lengths would provide a better understanding of the impact of alignment of chitosan and PCL molecules on blend properties.

5. Conclusions

In summary, chitosan was antibacterial on its surface to both Gram-positive and Gram-negative bacteria. Blending chitosan with PCL minimized the antibacterial property despite no chemical reaction between chitosan and PCL in the prepared blends. However, the degree of crystallinity of PCL was reduced and the surface roughness was significantly increased at the nanoscale. In light of the results obtained previously with eukaryotes, it maybe concluded that rougher surfaces may be more conducive to cellular and bacterial colonization.

Acknowledgment. Financial support for this research was provided by the Oklahoma Center for Advancement of Science and Technology (#HR05-075R). Guidance from Dr. Susheng Tan and Ms. Rangarani Karnati of the Chemistry Department of OSU in AFM and FTIR analyses respectively, is deeply appreciated.

CDV

References and Notes

(1) Ng, K. W.; Khor, H. L.; Hutmacher, D. W. *Biomaterials* **2004**, *25* (14), 2807−2818.
(2) Ouattar, B.; Simard, R. E.; Piett, G.; Begin, A.; Holley, R. A. *Int. J. Food Microbiol.* **2000**, *62* (1−2), 139−48.
(3) Madihally, S. V.; Matthew, H. W. *Biomaterials* **1999**, *20* (12), 1133−42.
(4) Ma, J.; Wang, H.; He, B.; Chen, J. *Biomaterials* **2001**, *22* (4), 331−336.
(5) Suh, J. K. F.; Matthew, H. W. T. *Biomaterials* **2000**, *21* (24), 2589−2598.
(6) Elcin, A. E.; Elcin, Y. M.; Pappas, G. D. *Neurol. Res.* **1998**, *20* (7), 648−654.
(7) Singla, A.; Lee, C. H. *J. Biomed. Mater. Res.* **2002**, *60* (3), 368−74.
(8) Elcin, Y. M.; Dixit, V.; Gitnick, G. *Artific. Organs* **1998**, *22* (10), 837−846.
(9) Muzzarelli, R.; Biagini, G.; Pugnaloni, A.; Filippini, O.; Baldassarre, V.; Castaldini, C.; Rizzoli, C. *Biomaterials* **1989**, *10* (9), 598−603.
(10) Park, J. S.; Choi, S. H.; Moon, I. S.; Cho, K. S.; Chai, J. K.; Kim, C. K. *J. Clin. Periodontol.* **2003**, *30* (5), 443−53.
(11) Yeo, Y. J.; Jeon, D. W.; Kim, C. S.; Choi, S. H.; Cho, K. S.; Lee, Y. K.; Kim, C. K. *J. Biomed. Mater. Res. B Appl. Biomater.* **2005**, *72* (1), 86−93.
(12) Muzzarelli, R.; Tarsi, R.; Filippini, O.; Giovanetti, E.; Biagini, G.; Varaldo, P. E. *Antimicrob. Agents Chemother.* **1990**, *34* (10), 2019−2023.
(13) Choi, B. K.; Kim, K. Y.; Yoo, Y. J.; Oh, S. J.; Choi, J. H.; Kim, C. Y. *Int. J. Antimicrob. Agents* **2001**, *18* (6), 553−7.
(14) Ikinci, G.; Senel, S.; Akincibay, H.; Kas, S.; Ercis, S.; Wilson, C. G.; Hincal, A. A. *Int. J. Pharm.* **2002**, *235* (1−2), 121−127.
(15) Fujita, M.; Kinoshita, M.; Ishihara, M.; Kanatani, Y.; Morimoto, Y.; Simizu, M.; Ishizuka, T.; Saito, Y.; Yura, H.; Matsui, T.; Takase, B.; Hattori, H.; Kikuchi, M.; Maehara, T. *J. Surg. Res.* **2004**, *121* (1), 135−140.
(16) Jockenhoevel, S.; Chalabi, K.; Sachweh, J. S.; Groesdonk, H. V.; Demircan, L.; Grossmann, M.; Zund, G.; Messmer, B. J. *Thorac. Cardiovasc. Surg.* **2001**, *49* (5), 287−90.
(17) Lucinda-Silva, R. M.; Evangelista, R. C. *J. Microencapsul.* **2003**, *20* (2), 145−52.
(18) Huang, Y.; Onyeri, S.; Siewe, M.; Moshfeghian, A.; Madihally, S. V. *Biomaterials* **2005**, *26* (36), 7616−27.
(19) Ma, L.; Gao, C. Y.; Mao, Z. W.; Zhou, J.; Shen, J. C.; Hu, X. Q.; Han, C. M. *Biomaterials* **2003**, *24* (26), 4833−4841.
(20) Khoo, C. G. L.; Frantzich, S.; Rosinski, A.; Sjostrom, M.; Hoogstraate, J. *Eur. J. Pharm. Biopharm.* **2003**, *55* (1), 47−56.
(21) Sarasam, A.; Madihally, S. V. *Biomaterials* **2005**, *26* (27), 5500−8.
(22) Coombes, A. G.; Rizzi, S. C.; Williamson, M.; Barralet, J. E.; Downes, S.; Wallace, W. A. *Biomaterials* **2004**, *25* (2), 315−25.
(23) Amass, W., A. A.; Tighe, B. *Polym. Int.* **1998**, *47*, 89−144.
(24) Bastioli, C.; Cerutti, A.; Guanella, I.; Romano, G. C.; Tosin, M. *J. Environ. Polym. Degrad.* **1995**, *3* (2), 81−95.
(25) Zhu, Y.; Gao, C.; Liu, X.; Shen, J. *Biomacromolecules* **2002**, *3* (6), 1312−9.
(26) Cascone, M. G.; Barbani, N.; Cristallini, C.; Giusti, P.; Ciardelli, G.; Lazzeri, L. *J. Biomater. Sci. Polym. Ed.* **2001**, *12* (3), 267−81.
(27) Banas, J. A. *Front. Biosci.* **2004**, *9*, 1267−77.
(28) Chaves, E. S.; Jeffcoat, M. K.; Ryerson, C. C.; Snyder, B. *J. Clin. Periodontol.* **2000**, *27* (12), 897−903.
(29) Shigemasa, Y.; Saito, K.; Sashiwa, H.; Saimoto, H. *Int. J. Biol. Macromol.* **1994**, *16* (1), 43−9.
(30) Davies, R. C.; Neuberger, A.; Wilson, B. M. *Biochim. Biophys. Acta* **1969**, *178* (2), 294−305.
(31) Chandy, T., S. P. *Biomat., Art. Cells, Art. Org.* **1990**, *18* (1), 1−24.
(32) C, W. *Polymer* **2005**, *46*, 147−155.
(33) Raghavan, D.; Kropp, B. P.; Lin, H. K.; Zhang, Y.; Cowan, R.; Madihally, S. V. *J. Biomed. Mater. Res. A* **2005**, *73* (1), 90−6.
(34) Pawlak, A.; Mucha, A. *Thermochim. Acta* **2003**, *396* (1−2), 153−166.
(35) Elzein, T.; Nasser-Eddine, M.; Delaite, C.; Bistac, S.; Dumas, P. *J. Colloid Interface Sci.* **2004**, *273* (2), 381−387.
(36) Pavia, D. L.; Lampman, G. M.; Kriz, G. S., Jr. *Introduction to Spectroscopy*, 3rd ed.; Harcourt College Publishers: Fort Worth, TX, 2000.
(37) Min, B.; Lee, S.; Lim, J.; You, Y.; Lee, T.; Kang, P.; Park, W. *Polymer* **2004**, *45* (21), 7137−7142.
(38) Piacibello, W.; Sanavio, F.; Garetto, L.; Severino, A.; Bergandi, D.; Ferrario, J.; Fagioli, F.; Berger, M.; Aglietta, M. *Blood* **1997**, *89* (8), 2644−53.
(39) No, H. K.; Park, N. Y.; Lee, S. H.; Meyers, S. P. *Int. J. Food Microbiol.* **2002**, *74* (1−2), 65−72.
(40) Balgude, A. P.; Yu, X.; Szymanski, A.; Bellamkonda, R. V. *Biomaterials* **2001**, *22* (10), 1077−84.
(41) Ranucci, C. S.; Kumar, A.; Batra, S. P.; Moghe, P. V. *Biomaterials* **2000**, *21* (8), 783−93.
(42) Rajnicek, A.; Britland, S.; McCaig, C. *J. Cell Sci.* **1997**, *110* (Pt 23), 2905−13.
(43) Curtis, A.; Wilkinson, C. *Biochem. Soc. Symp.* **1999**, *65*, 15−26.
(44) VandeVord, P. J.; Matthew, H. W.; DeSilva, S. P.; Mayton, L.; Wu, B.; Wooley, P. H. *J. Biomed. Mater. Res.* **2002**, *59* (3), 585−90.
(45) Cha, Y.; Pitt, C. G. *Biomaterials* **1990**, *11* (2), 108−112.
(46) Tomihata, K.; Ikada, Y. *Biomaterials* **1997**, *18* (7), 567−575.
(47) Senda, T.; He, Y.; Inoue, Y. *Polym. Int.* **2002**, *51* (1), 33−39.
(48) Tangpasuthadol, V.; Pongchaisirikul, N.; Hoven, V. P. *Carbohydr. Res.* **2003**, *338* (9), 937−942.
(49) Mao, J. S.; Cui, Y. L.; Wang, X. H.; Sun, Y.; Yin, Y. J.; Zhao, H. M.; De Yao, K. *Biomaterials* **2004**, *25* (18), 3973−81.
(50) Huang, Y.; Siewe, M.; Madihally, S. V. *Biotechnol. Bioeng.* **2006**, *93* (1), 64−75.

BM050935D